UDC 539.4

FEM Simulation of the Cross-Wedge Rolling Process for a Stepped Shaft

Z. Pater,[1] J. Tomczak,[2] and T. Bulzak[3]

Lublin University of Technology, Lublin, Poland

[1] z.pater@pollub.pl

[2] j.tomczak@pollub.pl

[3] t.bulzak@pollub.pl

The paper presents the results of numerical modeling of a cross-wedge rolling process for producing a stepped shaft. The modeling was performed with commercial software Forge NxT 1.1 using the finite element method. The numerical analysis enabled the determination of changes in the shape of the workpiece, effective strain, damage function and temperature distributions, as well as variations in the forces and torque acting on the tool. The numerical results demonstrate that personal computers can today be used to model even the most difficult cases of the cross-wedge rolling process, in which complex shapes of the tools and thermal phenomena occurring during the forming process have to be taken into consideration.

Keywords: cross-wedge rolling, stepped shaft, tools design, numerical simulation, finite element method.

Introduction. Cross-wedge rolling (CWR) belongs to the class of modern metalworking processes, which have recently been gaining in popularity. This method is mainly used in the production of stepped axles and shafts as well as preforms for drop forging [1, 2].

CWR has several advantages, including high efficiency, good material utilization, good strength properties of the products formed, environmental friendliness, low energy consumption and easy automation [1, 2]. Despite these merits, CWR is not used as broadly as it could in the manufacture of machine parts. This is mainly due to difficulties in designing tools that would guarantee the accuracy of the rolling process. Even a slight change in wedge angles may lead to problems such as uncontrolled slip, necking (fracture) of the rolled product, or material cracking. Therefore, the design work related to launching new CWR-based technologies is usually only done by designer teams employed by roller machine producers. Even in this case, however, the final design (for products of more complex shapes) is obtained via successive approximations, using the trial and error method. As a result, the design and production of tools that can guarantee the expected quality of rolled products is a time-consuming and costly process, which obviously has an impact on the number of new implementations. This situation is expected to improve with the widespread use of numerical techniques which allow modeling of complex metalworking processes under three-dimensional strain. Numerical models make it possible to validate the accuracy of a design in the virtual space of the computer, by simulating the forming process. If the results are unsatisfactory, appropriate changes can be introduced to tool design and the simulations can be repeated until an acceptable result is obtained.

CWR is one of the hardest metalworking processes to model numerically. This is caused by the complex shape of the products, very large tool pitch (many times larger than the dimensions of the workpiece), a complex interaction between the tool and the material being formed (both slip and clinging of material can occur), and nonlinearities. Due to all these facts, the CWR process was first successfully modeled using the finite element method (FEM) as late as the end of the last century. Specialized literature offers numerous examples of simulations of the CWR process performed using the following

commercial programs: ANSYS/LS-DYNA [3–24], DEFORM-3D [25–65], Forge3 [66–69], MSC.SuperForm, MARC.AutoForge, and Simufact.Forming [70–81]. Most of these analyses have focused on the stability of rolling and determining the impact of the main parameters of the process on the possibility of occurrence of defects. FEM has also been used to analyze temperature distributions, microstructures, and stress-strain states of rolled products. However, these analyses have been limited to simple cases of rolling, in which often only a single reduction in the cross section of the product was being formed.

Currently, it is possible to model even very complex cases of CWR using a PC. This means that this interesting metal forming method can be developed using virtual prototyping. The aim of this paper is to demonstrate this claim using the example of numerical analysis of CWR of a stepped shaft. It must be emphasized that the process of forming a stepped shaft, which has been selected for numerical simulation, fully reflects the potential of cross-wedge rolling, which, we believe, should have a much broader use than it has today.

Model of the CWR Process for a Stepped Shaft. Numerical simulations of the CWR process were performed using the stepped shaft shown in Fig. 1, which had a more complex shape than the shafts investigated in previous studies [3–81]. It was assumed that the shaft would be formed by two wedge rollers (nominal diameter 800 mm) from a $\varnothing 72\times 110$ mm billet, whose diameter was equal to that of the head of the forging. In this situation, the shaft journals were to be formed at deformation ratios δ (a measure of plastic strain in CWR, where $\delta = d_0/d$, d_0 is the diameter of the billet and d is the diameter of the step being rolled) reaching 3.33. Such a large reduction in diameter cannot be achieved in one working cycle (a single pass of the wedges), and so forming must be done in two operations (first the billet is rolled to an intermediate diameter and then to the target diameter).

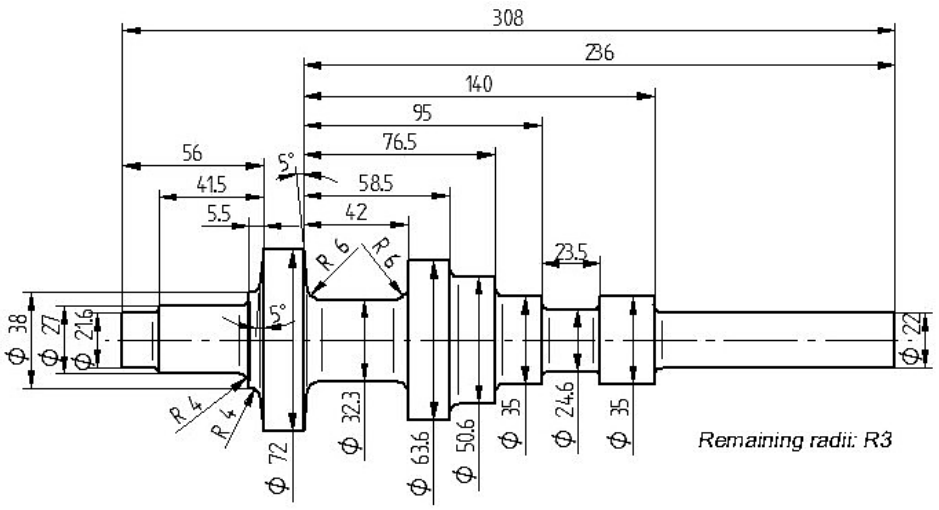

Fig. 1. Stepped shaft used in the numerical analysis.

Figure 2 shows an unfolded view of the wedge tool (diameter 800 mm) used in the cross wedge rolling of the stepped shaft. This figure also shows the overall dimensions of the tool and the wedge spreading angles β (wedge geometry is described by two angles: spreading angle β and forming angle α, defining the inclination of the wedge's side wall; in the case studied $\alpha = 22.5°$). To obtain the desired shape of the shaft, it was necessary to use a rolling scenario in which the excess stock (end faces with funnels formed in them) was cut off from the product.

The analysis of CWR of the stepped shaft was carried out using the Forge NxT 1.1 commercial software package. Figure 3 shows a FEM model of the investigated CWR

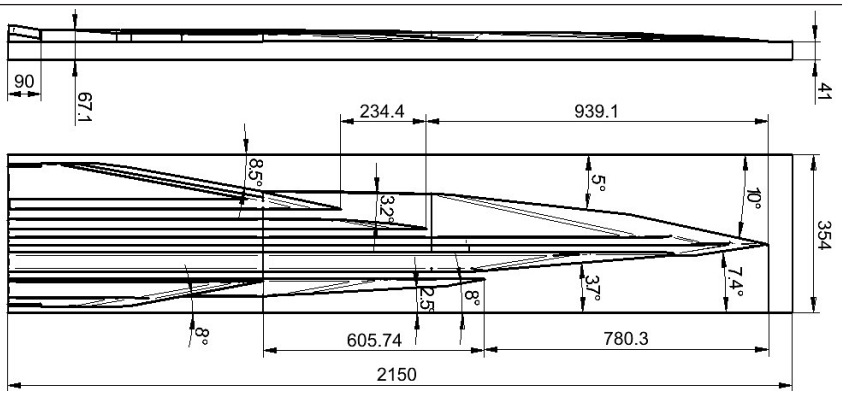

Fig. 2. An unfolded view of the wedge segment used for the rolling of the stepped shaft shown in Fig. 1 with marked wedge spreading angles β; wedge diameter 800 mm.

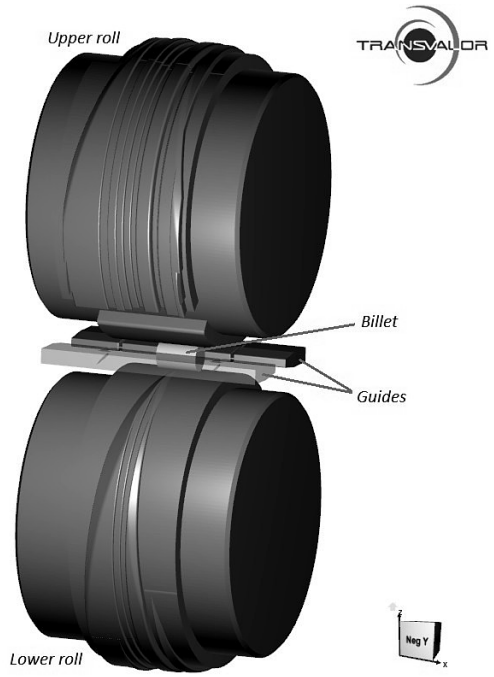

Fig. 3. Geometrical model of rolling a stepped shaft generated using Forge NxT 1.1 software.

process developed for computational purposes. The model consists of two wedge segments (with a shape described using triangular surface elements), two guiding bars (guides) (for holding the workpiece in the working space of the rollers), and a cylindrical billet ∅72×110 mm. Geometric models of the tools were imported from the Solid Edge CAD system, in which they had been designed.

The product being formed was modeled using 4-node tetrahedral elements. Because of the intense deformation of the metal, leading to considerable distortion of the final-element grid, the grid rearrangement option was used in the calculations. It was enabled when the increase in the strain in an element was larger 0.5. As a result, both the number of nodes (in the range 9500–42,500) and the number of elements (42,500–165,000) used in the calculations were changed (Fig. 4). The entire rolling process was divided into 4200 computational steps, and the computation time on a 32-core computer was 61 hours.

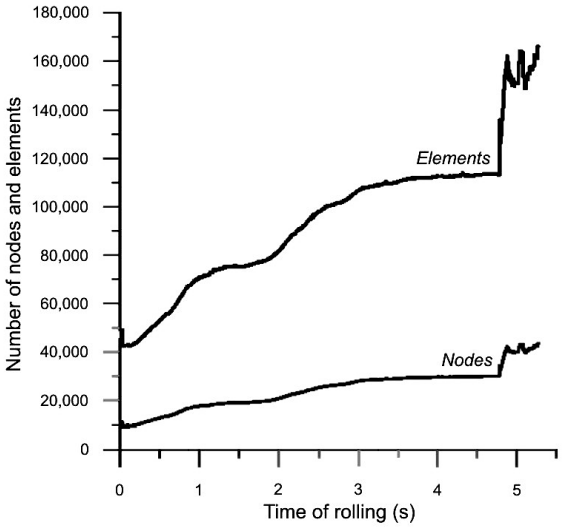

Fig. 4. Changes in the number of elements and nodes used in numerical calculations as a function of rolling time.

It was assumed that the shaft was made of 19MnCr5 grade steel, a model of which was obtained from the Forge NxT 1.1 library. The remaining parameters used in the calculations were as follows: friction coefficient on the material–tool contact surface $m = 1$ for wedges and $m = 0.2$ for guides, roller rotational speed 10 rpm, billet temperature 1170°C, tool temperature 250°C, heat transfer coefficient between material and tools 10 kW/(m^2 · K), and heat transfer coefficient between material and surroundings 200 W/(m^2 · K).

Selected Calculation Results. FEM allows precise tracking of changes in product shape during the rolling of the analyzed stepped shaft. The changes are shown in Fig. 5. In the initial phase of the process, the wedge tools sink into the middle of the billet to reduce its diameter. Once the two middle steps of the shaft have been formed, the smaller diameter step downs located further to the shaft end, with diameters of 32.3 and 35 mm are rolled. Then the head is formed. The tools used for rolling this portion of the forging were the most difficult to design, because it was necessary to define the moment when the wedge cuts into the material (this moment determines what volume of material will fill the space between the wedges), which required correcting the design and repeating the calculations several times. In further parts of the process, the smallest-diameter steps are formed with the simultaneous loosening of the already formed middle steps. Next, the shaft is subjected to final sizing in order to remove any shape errors that may have arisen in the previous phases of the rolling process. At the end of the forming process, the unprocessed stock is cut off from the ends of the product. Throughout the rolling process, the forging rotates securely and there is no danger of uncontrolled slipping.

Figure 6 shows how the temperature is distributed in the rolled stepped shaft. Despite the relatively long forming time ($t \approx 5.2$ s) during which the shaft was in contact with the tools, which have a much lower temperature ($T = 250$°C), no drop in material temperature below the lower limit for metal forming was observed. The temperature of the metal was the lowest in the middle steps of the shaft, which are formed in the initial phase of the process and then, being rolled over the surfaces of the rollers, transfer the heat to the latter. By contrast, the temperature in the inner layers of the shaft did not decrease significantly; on the contrary, an increase was observed in some places. It is assumed that in these portions of the product, the heat transferred to the tools during the heat exchange is compensated by the heat generated by deformation and friction work.

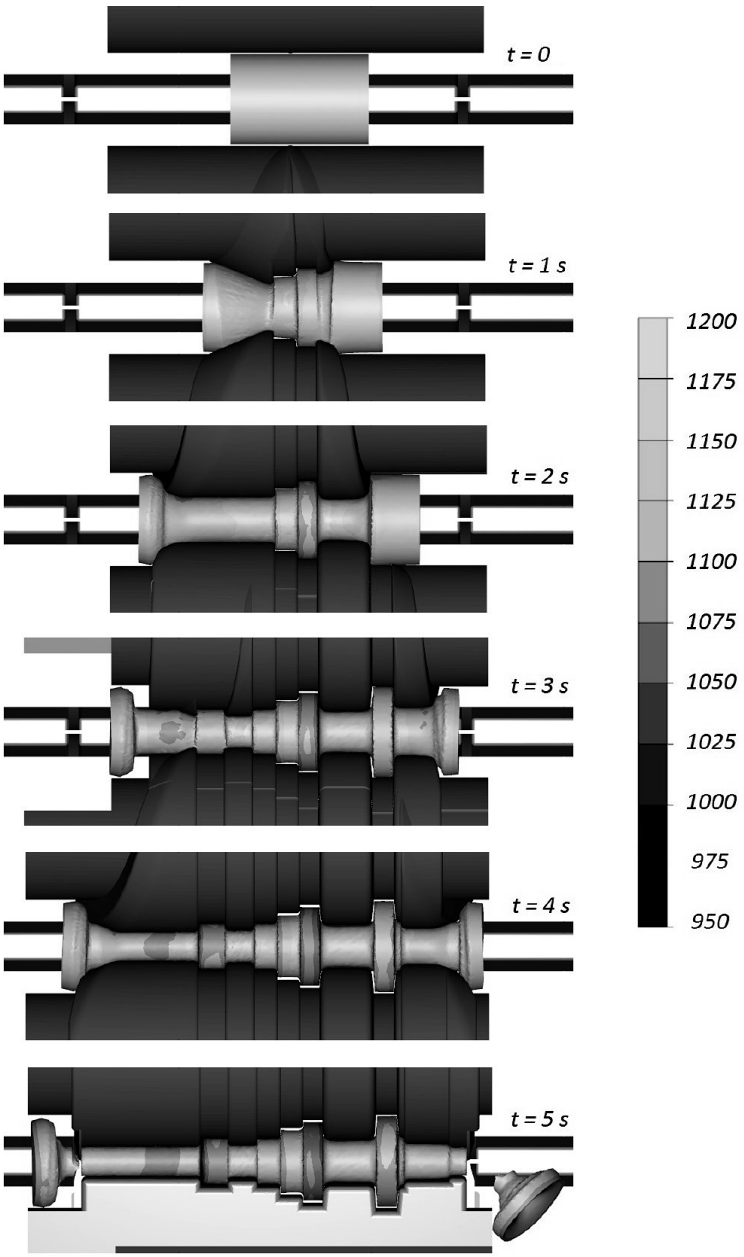

Fig. 5. A Forge NxT 1.1 simulation of the course of the rolling process for a stepped shaft, with colour-coded temperature distribution (in ℃).

Figure 7 shows the distribution of effective strain in the rolled stepped shaft. The data in this figure indicate that strain increases with the reduction in diameter, with the strain in the surface layers being higher than in the axial zone. This is the effect of the friction forces acting on the material–tool contact surface. At the same time, it should be noted that the strain in the shaft is very high, which cannot be the result of the reduction in diameter alone. This fact can be explained by the intense flow of metal in the tangential direction (mainly due to friction forces), which is characteristic of CWR and leads to the formation of redundant strain in the metal.

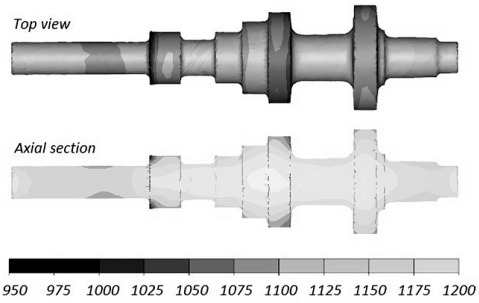

Fig. 6

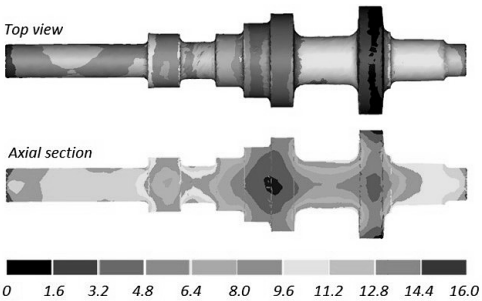

Fig. 7

Fig. 6. Temperature distribution in the stepped shaft (in ℃) determined using Forge NxT 1.1.
Fig. 7. Effective strain distribution determined using Forge NxT 1.1.

One of the common defects of CWR-formed products is internal cracking in the axial zone (the Mannesmann effect). The crack formation can be predicted on the basis of an analysis of the fracture (damage) function, calculated from the Cockroft–Latham ductile fracture criterion. The fracture function for the investigated rolling process is shown in Fig. 8. The data in this figure demonstrate that the extreme steps of the shaft, in which there is a significant twisting of the material, are the most vulnerable to fracture. At the same time, no increase in the fracture function in the axial zone of the formed shaft was observed, indicating that the Mannesmann effect should not occur in the investigated shaft.

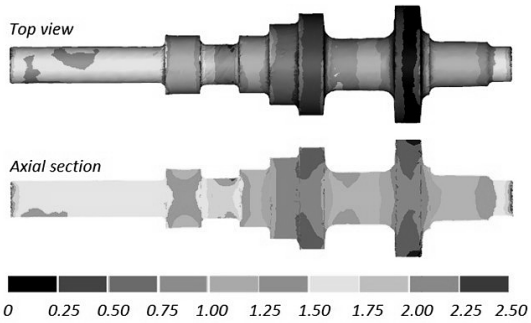

Fig. 8. Distribution of damage function, according to the Cockroft–Latham criterion, determined using Forge NxT 1.1.

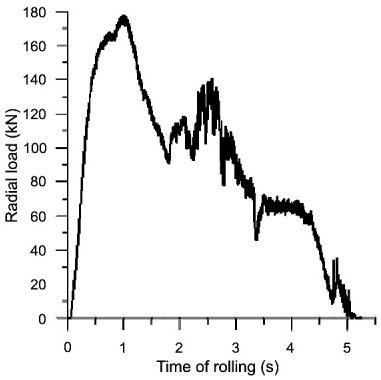

Fig. 9

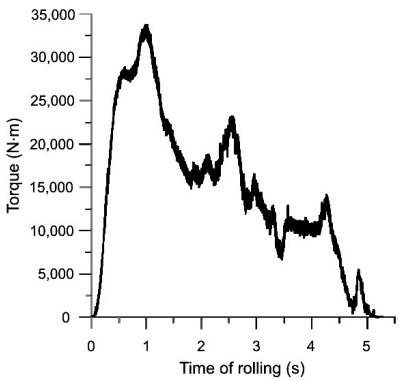

Fig. 10

Fig. 9. Distribution of radial load during forming of the analyzed stepped shaft.
Fig. 10. Distribution of torque acting on the roller during forming of the analyzed stepped shaft.

The distributions of two selected strength parameters of the rolling process, i.e., radial force (perpendicular to the tool surface) and torque (which pushes the roller in the rolling direction) are shown in Figs. 9 and 10, respectively. An analysis of the data given in these figures demonstrates that both torque and radial force have the highest values in the initial forming phase of the CWR process. It is at this stage that the contact surface between the material and the tools is the largest. The smallest values of force parameters (several times smaller than in the forming stages) are observed in the sizing phase.

Conclusions. This paper describes a thermo-mechanical model of cross-wedge rolling of a stepped shaft. This model was used to perform a numerical simulation of rolling of the analyzed shaft with the commercial software package Forge NxT 1.1. The calculations were done to determine the successive changes in the shape of the shaft, temperature and strain distributions, and the fracture criterion for the shaft. Also, distributions of radial force and torque acting on the shaft during the rolling process were calculated. It was found that a PC equipped with commercial software, such as Forge NxT 1.1, is sufficient to successfully model such complex metal forming processes as cross-wedge rolling. This means that design work related to launching new manufacturing processes based on the modern CWR technology can be made easier by the application of numerical modeling. This is especially important for individuals who are new to the CWR technology.

Acknowledgments. This scientific work was funded from the research and education (statutory activity) fund granted by the Polish Ministry of Science and Higher Education to the Faculty of Mechanical Engineering of the Lublin University of Technology.

1. Z. Pater, "Cross-wedge rolling," in: S. Hashmi (Ed.), *Comprehensive Materials Processing*, Vol. 3, Elsevier (2014), pp. 211–279.
2. X. P. Fu and T. A. Dean, "Past developments, current applications and trends in the cross wedge rolling process," *Int. J. Mach. Tool. Manu.*, **33**, No. 2, 367–400 (1993).
3. Y. Dong, K. A. Tagavi, and M. R. Lovell, "Analysis of interfacial slip in cross-wedge rolling: a numerical and phenomenological investigation," *J. Mater. Process. Tech.*, **97**, Nos. 1–3, 44–53 (2000).
4. M. R. Lovell, "Evaluation of critical interfacial friction in cross wedge rolling," *J. Tribol.*, **123**, No. 2, 424–429 (2001).
5. Y. Dong, M. Lovell, and K. Tagavi, "Analysis of interfacial slip in cross-wedge rolling: an experimentally verified finite-element model," *J. Mater. Process. Tech*., **80–81**, 273–281 (1998).
6. Y. Dong, K. A. Tagavi, M. R. Lovell, and Z. Deng, "Analysis of stress in cross wedge rolling with application to failure," *Int. J. Mech. Sci.*, **42**, 1233–1253 (2000).
7. Z. Deng, M. R. Lovell, and K. A. Tagavi, "Influence of material properties and forming velocity on the interfacial slip characteristics of cross wedge rolling," *J. Manuf. Sci. Eng.*, **123**, 647–653 (2001).
8. S. G. Choi, D. J. Yoon, G. A. Lee, et al., "Cold rolling technique for eliminating cutting process in manufacturing precise product using non-heat-treated micro alloys," *Mater. Sci. Forum*, **475–479**, 3235–3238 (2005).
9. Q. Li and M. Lovell, "On the interfacial friction of a two-roll CWR process," *J. Mater. Process. Tech.*, **160**, 245–256 (2005).
10. S. Urankar, M. Lovell, C. Morrow, et al., "Establishment of failure conditions for cross-wedge rolling of hollow shafts," *J. Mater. Process. Tech.*, **177**, 545–549 (2006).
11. S. Urankar, M. Lovell, C. Morrow, et al., "Development of a critical friction model for cross wedge rolling hollow shafts," *J. Mater. Process. Tech.*, **177**, 539–544 (2006).

12. S. Xuedao, L. Chuanmin, Z. Jing, and H. Zhenghuan, "Theoretical and experimental study of varying rule of rolling-moment about cross-wedge rolling," *J. Mater. Process. Tech.*, **187–188**, 752–756 (2007).
13. H. W. Lee, G. A. Lee, D. J. Yoon, et al., "Optimization of design parameters using a response surface method in a cold cross-wedge rolling," *J. Mater. Process. Tech.*, **201**, 112–117 (2008).
14. X. Shu, X. Wei, Ch. Li, and Z. Hu, "The influence rules of stress about technical parameters on synchronous rolling railway axis with multi-wedge cross-wedge rolling," *Appl. Mech. Mater.*, **37–38**, 1482–1488 (2010).
15. J. Zhao and L. Lu, "The application of multi-wedge cross wedge rolling forming long shaft technology," *Appl. Mech. Mater.*, **101–102**, 1002–1005 (2012).
16. V. Y. Shchukin, G. V. Kozhevnikova, and V. V. Petrenko, "Cross-wedge rolling at Pti NAS Belarus," *Appl. Mech. Mater.*, **201–202**, 1198–1202 (2012).
17. W. Peng and K. Zhang, "Theoretical research of the axial force about cross wedge rolling," *Key Eng. Mater.*, **433**, 27–32 (2010).
18. X. Xing and X. Shu, "Finite element analysis of stress and strain in two-wedge cross wedge rolling step-shaft part," *Mater. Sci. Forum*, **575–578**, 255–260 (2008).
19. C. Yang, K. Zhang, and Z. Hu, "Development of central minute cavity in the workpiece of cross wedge rolling," *Appl. Mech. Mater.*, **215–216**, 766–770 (2012).
20. X. Shu, B. Sun, and M. Xiao, "Influence regularities of axial force of cross wedge rolling symmetric shaft-parts about technical parameters," *Adv. Mater. Res.*, **314–316**, 589–593 (2011).
21. H. N. Lu, D. B. Wei, and Z. Y. Jiang, "Investigation on dimensional accuracy in micro cross wedge rolling of metals," *Key Eng. Mater.*, **622–623**, 943–948 (2014).
22. D. Wei, H. Lu, Z. Jiang, and K. Manabe, "Optimization of micro cross wedge rolling and surface morphology of micro stepped components," *Key Eng. Mater.*, **622–623**, 964–969 (2014).
23. Z. Jiang, H. Lu, D. Wei, et al., "Finite element method analysis of micro cross wedge rolling of metals," *Procedia Engineer.*, **81**, 2463–2468 (2014).
24. W. F. Peng, J. H. Zhang, G. X. Huang, et al., "Stress distribution during the cross-wedge rolling of composite 42CrMo/Q235 laminated shafts," *Int. J. Adv. Manuf. Tech.*, **83**, 145–155 (2016).
25. M. Wang, X. Li, and F. Du, "Analysis of metal forming in two-roll cross wedge rolling process using finite element method," *J. Iron Steel Res. Int.*, **16**, No. 1, 38–43 (2009).
26. X. Li, M. Wang, and F. Du, "The coupling thermal-mechanical and microstructural model for the FEM simulation of cross wedge rolling," *J. Mater. Process. Tech*., **172**, 202–207 (2006).
27. Y. Xiong, S. Sun, Y. Li, et al., "Effect of warm cross-wedge rolling on microstructure and mechanical property of high carbon steel rods," *Mater. Sci. Eng. A*, **431**, 152–157 (2006).
28. M. Wang, X. Li, F. Du, and Y. Zheng, "A coupled thermal-mechanical and microstructural simulations of the cross wedge rolling process and experimental verification," *Mater. Sci. Eng. A*, **391**, 305–312 (2005).
29. M. Wang, X. Li, F. Du, and Y. Zheng, "Hot deformation of austenite and prediction of microstructure evolution of cross-wedge rolling," *Mater. Sci. Eng. A*, **379**, 133–140 (2004).

30. G. Fang, L. P. Lei, and P. Zeng, "Three-dimensional rigid-plastic finite element simulation for two-roll cross-wedge rolling process," *J. Mater. Process. Tech.*, **129**, 245–249 (2002).
31. W. Regone, M. da Silva, and S. Button, "Numerical and experimental analysis of the microstruc¬tural evolution during cross wedge rolling of V-Ti microalloyed steel," *REM - Revista Escola de Minas (Metalurgia & Materials)*, **62**, No. 4, 495–502 (2009).
32. C. G. Xu, G. H. Liu, G. S. Ren, et al., "Finite element analysis of axial feed bar rolling," *Acta Metall. Sin. - Engl.*, **20**, No. 4, 463–468 (2007).
33. S. J. Mirhamadi, M. Hamedi, and S. Ajami, "Investigating the effects of cross wedge rolling tool parameters on formability of Nimonic® 80A and Nimonic® 115 superalloys," *Int. J. Adv. Manuf. Tech*., **74**, 995–1004 (2014).
34. F. Shen, W. Yu, W. Peng, et al., "The strain analysis of plate cross wedge rolling of spiral shaft parts," *Adv. Mater. Res.*, **941–944**, 1895–1900 (2014).
35. C. Yang, K. Zhang, and Z. Hu, "Simulation analysis of cross wedge rolling hollow parts with mandrel," *Adv. Mater. Res*., **538–541**, 542–547 (2012).
36. B. Hu, X. Shu, P. Yu, and W. Peng, "The strain analysis at the broadening stage of the hollow railway axle by multi-wedge cross wedge rolling," *Appl. Mech. Mater.*, **494–495**, 457–460 (2014).
37. J. Zhou, Z. Yu, and Q. Zeng, "Analysis and experimental studies of internal voids in multi-wedge cross wedge rolling stepped shaft," *Int. J. Adv. Manuf. Tech.*, **72**, 1559–1566 (2014).
38. H. Yan, L. Wang, Y. Liu, et al., "Effect of thread helix angle on the axial metal flow of cross wedge rolling thread shaft," *Appl. Mech. Mater.*, **440**, 177–181 (2014).
39. Z. Zheng, B. Wang, and Z. Hu, "Study on roller profile for cam forming by cross wedge rolling," *Appl. Mech. Mater.*, **217–219**, 1713–1718 (2012).
40. F. Ying, J., Shen, and L. Wu, "Study on the process of gear shaft formed by cross wedge rolling based on deform," *Adv. Mater. Res.*, **497**, 55–60 (2012).
41. X. Shu, X. Wei, and L. Chen, "Influence analysis of block wedge on rolled-piece end quality in cross wedge rolling," *Appl. Mech. Mater.*, **101–102**, 1055-1058 (2012).
42. X. Wei and X. Shu, "Study on production mechanism of end concavity in cross wedge rolling," *Adv. Mater. Res.*, **314–316**, 468–472 (2011).
43. P. Qui, H. Xiao, and M. Li, "Effect of non-uniform temperature field on piece rolled by three-roll cross wedge rolling," *Appl. Mech. Mater.*, **16–19**, 456–461 (2009).
44. J. Zhou, C. Xiao, Y. Yu, and Z. Jia, "Influence of tool parameters on central deformation in two-wedge two-roll cross-wedge rolling," *Adv. Mater. Res.*, **486**, 478–483 (2012).
45. H. Yan, J. Liu, Z. Hu, et al., "Effects of die tooth profile on forming helical tooth shaft in cross wedge rolling," *Appl. Mech. Mater.*, **274**, 165–169 (2013).
46. W. Ma, B. Wang, J. Zhou, and Q. Li, "Analysis of square billet cross wedge rolling process using finite element method," *Appl. Mech. Mater.*, **271–272**, 406–411 (2013).
47. M. Jin, J. Li, and F. Ying, "Study on influencing factors of tooth forming quality for gear shaft with cross wedge rolling," *Appl. Mech. Mater*., **201–202**, 1164–1169 (2012).
48. F. Zhao, J. Liu, J. Huang, and Z. Hu, "Analysis of the wedge tip fillet for central defects in the process of cross wedge rolling 4Cr9Si2 valve," *Adv. Mater. Res*., **706–708**, 3–6 (2013).

49. B. Sun, X. Zeng, X. Shu, et al., "Feasibility Study on forming hollow axle with multi-wedge synchrostep by cross wedge rolling," *Appl. Mech. Mater.*, **201–202**, 673–677 (2012).
50. X. Shu, Z. Li, and W. Zu, "Bending analysis and measures of the forming of automobile semi-axle on cross-wedge rolling with multi-wedge," *Appl. Mech. Mater.*, **184–185**, 75–79 (2012).
51. X. Wang, K. Zhang, J. Liu, and Z. Hu, "The effect and experimental research of forming angle on internal defect of valve roughcast formed by single cross wedge rolling," *Adv. Mater. Res.*, **230–232**, 389–394 (2011).
52. W. Gong, X. Shu, W. Peng, and B. Sun, "The research on the microstructure evolution law of cross wedge rolling asymmetric shaft-parts based on parity wedge," *Appl. Mech. Mater.*, **201–202**, 1121–1125 (2012).
53. Z. Pater, "Numerical modelling of cross wedge rolling of rotary cutter body," *Acta Mechanica Slovaca*, No. 3A, 361–366 (2008).
54. Z. Pater, A. Gontarz, G. Samołyk, et al., "Analysis of cross rolling process of toothed titanium shafts," *Arch. Metall. Mater.*, **54**, No. 3, 617–626 (2009).
55. Z. Pater, A. Gontarz, and A, Tofil, "Analysis of the cross-wedge rolling process of toothed shafts made from 2618 aluminium alloy," *J. Shanghai Jiaotong Univ. (Science)*, **16**, No. 2, 162–166 (2011).
56. Y. Huo, Q. Bai, B. Wang, et al., "A new application of unified constitutive equations for cross wedge rolling of high-speed railway axle steel," *J. Mater. Process. Tech.*, **223**, 274–283 (2015).
57. H. Ji, J. Liu, B. Wang, et al., "Cross-wedge rolling of a 4Cr9Si2 hollow valve: explorative experiment and finite element simulation," *Int. J. Adv. Manuf. Tech.*, **77**, 15–26 (2015).
58. H. Ji, J. Liu, B. Wang, et al., "Numerical analysis and experiment on cross wedge rolling and forging for engine valves," *J. Mater. Process. Tech.*, **221**, 233–242 (2015).
59. C. Yang and Z. Ku, "Research on the ovality of hollow shafts in cross wedge rolling with mandrel," *Int. J. Adv. Manuf. Tech.*, **83**, 67–76 (2016).
60. J. Ma, C. Yang, Z. Zheng, et al., "Influence of process parameters on the microstructural evolution of a rear axle tube during cross wedge rolling," *Int. J. Miner. Met. Mater.*, **23**, No. 11, 1302–1314 (2016).
61. W. Peng, S. Zheng, Y. Chiu, et al., "Multi-wedge cross wedge rolling process of 42CrMo4 large and long hollow shaft," *Rare Metal Mat. Eng.*, **45**, No. 4, 836–842 (2016).
62. X. D. Shu, J. Wei, and C. Liu, "Study on the control of end quality by one closed cross wedge rolling based wedge block," *Metalurgija*, **56**, Nos. 1–2, 123–126 (2017).
63. J. Huo, J. Lin, Q. Bai, et al., "Prediction of microstructure and ductile damage of a high-speed railway axle steel during cross wedge rolling," *J. Mater. Process. Tech.*, **239**, 359–369 (2017).
64. C. Yang, J. Ma, and Z. Hu, "Analysis and design of cross wedge rolling hollow axle sleeve with mandrel," *J. Mater. Process. Tech.*, **239**, 346–358 (2017).
65. H. Ji, J. Liu, B. Wang, et al., "A new method for manufacturing hollow valves via cross wedge rolling and forging: Numerical analysis and experiment validation," *J. Mater. Process. Tech.*, **240**, 1–11 (2017).
66. M. Meyer, M. Stonis, and B. A. Behrnes, "Cross wedge rolling preforms for crankshafts," *Key Eng. Mater.*, **504–506**, 205–210 (2012).

67. M. Meyer, M. Stonis, and B. A. Behrens, "Cross wedge rolling and bi-directional forging of preforms for crankshafts," *Prod. Eng*., **9**, 61–71 (2015).

68. M. F. Novella, A. Ghiotti, S. Bruschi, and P. F. Bariani, "Ductile damage modeling at elevated temperature applied to the cross wedge rolling of AA6082-T6 bars," *J. Mater. Process. Tech.*, **222**, 259–267 (2015).

69. K. Kpodzo, L. Fourment, P. Lanse, and P. Montmitonnet, "An accurate time integration scheme for arbitrary rotation motion: application to metal forming simulation," *Int. J. Mater. Form*., **9**, 71–84 (2016).

70. Z. Pater and A. Tofil, "Experimental and theoretical analysis of the cross-wedge rolling process in cold forming conditions," *Arch. Metall. Mater.*, **52**, No. 2, 289–297 (2007).

71. F. Q. Ying and B. S. Pan, "Analysis on temperature distribution in cross wedge rolling process with finite element method," *J. Mater. Process. Tech.*, **187–188**, 392–396 (2007).

72. Z. Pater and J. Bartnicki, "Finished cross-wedge rolling of hollowed cutters," *Arch. Metall. Mater.*, **51**, No. 2, 205–211 (2006).

73. Z. Pater, "Finite element analysis of cross wedge rolling," *J. Mater. Process. Tech.*, **173**, 201–208 (2006).

74. Z. Pater, A. Gontarz, and W. Weronski, "Cross-wedge rolling by means of one flat wedge and two shaped rolls," *J. Mater. Process. Tech.*, **177**, 550–554 (2006).

75. Z. Pater, J. Bartnicki, and G. Samołyk, "Numerical modelling of cross-wedge rolling process of ball pin," *J. Mater. Process. Tech*., **164–165**, 1235–1240 (2005).

76. J. Bartnicki and Z. Pater, "Numerical simulation of three-rolls cross-wedge rolling of hollowed shaft," *J. Mater. Process. Tech.*, **164–165**, 1154–1159 (2005).

77. Z. Pater, "The analysis of the strain in parts formed by means of the wedge-rolls rolling (WRR)," *Arch. Metall. Mater.*, **50**, No. 3, 675–690 (2005).

78. J. Bartnicki and Z. Pater, "The aspects of stability in cross-wedge rolling processes of hollowed shafts," *J. Mater. Process. Tech*., **155–156**, 1867–1873 (2004).

79. Z. Pater, "Stress state in cross wedge rolling process," *Arch. Metall.*, **48**, No. 1, 21–35 (2003).

80. Z. Pater, T. Bulzak, and J. Tomczak, "Cross-wedge rolling of driving shaft from titanium alloy Ti6Al4V," *Key Eng. Mater.*, **687**, 125–132 (2016).

81. H. Huang, X. Chen, B. Fan, et al., "Initial billet temperature influence and location investigation on tool wear in cross wedge rolling," *Int. J. Adv. Manuf. Tech*., **79**, 1545–1556 (2015).

Received 01. 09. 2017